 

Selected Paper

# Preparation, Structure, and Characterization of a Novel Diphosphoheptadecatungstate Complex, $[(P_2O_7)W_{17}O_{51}]^{4-}$

**Sadayuki Himeno,*[1] Tadashi Katsuta,[1] Masayo Takamoto,[1] and Masato Hashimoto[2]**

[1]Department of Chemistry, Faculty of Science, Kobe University, 1-1 Rokkodai, Nada-ku, Kobe 657-8501

[2]Department of Material Science and Chemistry, Faculty of Systems Engineering, Wakayama University, 930 Sakaedani, Wakayama 640-8510

Received June 23, 2005; E-mail: himeno@kobe-u.ac.jp

A novel diphosphoheptadecatungstate complex, $[(P_2O_7)W_{17}O_{51}]^{4-}$ was prepared from a 200 mM (M = mol dm$^{-3}$) W(VI)–10 mM $P_2O_7^{4-}$–0.6 M HCl–40% (v/v) $CH_3CN$ system, and characterized by IR, UV–vis, $^{31}$P NMR, and $^{183}$W NMR spectroscopy, and voltammetry. Single-crystal X-ray analysis was made on $[(C_2H_5)_4N]_4[(P_2O_7)W_{17}O_{51}]\cdot CH_3CN$, which crystallized in the monoclinic space group $P2_1/n$, with cell parameters $a = 16.1877(8)$, $b = 22.103(1)$, $c = 22.670(1)$ Å, $\beta = 90.847(1)^\circ$, $V = 8110.3(7)$ Å$^3$, and $Z = 4$. The anion consists of a $PW_8O_{31}$ fragment derived from a $\beta$-Keggin-type $[PW_{12}O_{40}]^{3-}$ structure, and two $PW_8O_{31}$ units are linked by five oxygen atoms and a $WO_5$ square pyramid. The $[(P_2O_7)W_{17}O_{51}]^{4-}$ anion exhibited a four-step reversible one-electron redox wave in $CH_3CN$, and a three-step two-electron redox wave resulted in the presence of acid. This is the first example of an electrochemically-active diphosphotungstate complex.

Heteropolyoxometalates have attracted great attention owing to their potential use in various fields of chemistry. To date, limited types of heteropolyoxometalates based on tetrahedral $XO_4$-type hetero-ions have received fundamental study. One of the major challenges in the polyoxometalate chemistry is the preparation of heteropoly complexes with new structural types. Since 1990, we have pursued the synthetic study of polyoxometalates incorporating diphosphate, because the hetero-ion possesses six oxygen atoms available for binding. First, we have synthesized $[(P_2O_7)Mo_{18}O_{54}]^{4-}$ in a Mo(VI)–$P_2O_7^{4-}$–$CH_3CN$ media.[1] Unlike the Dawson-type $[P_2Mo_{18}O_{62}]^{6-}$ anion, which consists of two A-type $PMo_9$ units, the $[(P_2O_7)Mo_{18}O_{54}]^{4-}$ anion has a structure based on two B-type $PMo_9$ units.[2] Later, we also found that the $[(P_2O_7)Mo_{18}O_{54}]^{4-}$ anion is spontaneously transformed first into $[H_6(P_2O_7)Mo_{15}O_{48}]^{4-}$,[3] and finally into $[H_{12}(P_2O_7)Mo_{12}O_{42}]^{4-}$ in aqueous-$CH_3CN$ media.[4] In an old study, Rosenheim and Schapiro also prepared diphosphododecamolybdate from an aqueous Mo(VI)–$P_2O_7^{4-}$ system.[5] According to Kortz, the $(n\text{-}C_4H_9)_4N^+$ ($n$-$Bu_4N^+$) salt of $[H_6(P_2O_7)Mo_{15}O_{48}]^{4-}$ was crystallized into a dimeric form of $[\{(P_2O_7)Mo_{15}O_{45}\}_2]^{8-}$ in $CH_3CN$.[6] Besides, Kortz prepared $[(P_2O_7)Mo_6O_{18}(H_2O)_4]^{4-}$ from aqueous media and structurally characterized it.[7] Of the diphosphomolybdates, $[(P_2O_7)Mo_{18}O_{54}]^{4-}$ and $[H_6(P_2O_7)Mo_{15}O_{48}]^{4-}$ are reported to be voltammetrically reducible.[1,3,8]

As far as diphosphotungstates are concerned, Kortz et al. also isolated $[(P_2O_7)_4W_{12}O_{36}]^{16-}$ from an aqueous W(VI)–$P_2O_7^{4-}$ system.[9] In spite of extensive studies, however, relatively little is known about diphosphotungstate complexes. This paper aimed at the preparation of a voltammetrically-active diphosphotungstate complex by using $CH_3CN$ as an auxiliary solvent, because the voltammetrically-active $[(P_2O_7)Mo_{18}O_{54}]^{4-}$ and $[H_6(P_2O_7)Mo_{15}O_{48}]^{4-}$ anions were prepared from Mo(VI)–$P_2O_7^{4-}$–$CH_3CN$ systems.[1,3] To the best of our knowledge, there are no known examples of voltammetrically-reducible diphosphotungstate complexes. As expected, we prepared a previously unknown diphosphoheptadecatungstate, $[(P_2O_7)W_{17}O_{51}]^{4-}$. The present paper reports on the first example of a voltammetrically-active diphosphotungstate complex.

## Experimental

**Crystallography.** A single crystal obtained as below was subjected to X-ray intensity collection on Rigaku Mercury CCD diffractometer at the Department of Chemistry, Faculty of Science, Kanazawa University, using graphite-monochromated Mo K$\alpha$ radiation (0.71069 Å) at 100(2) K. Tungsten atoms were located by a direct method and all other non-H atoms were found by successive differential Fourier syntheses. Hydrogen atoms were not included in the structural model. All non-H atoms were refined anisotropically by full-matrix calculations by SHELX97.[10] Crystallographic and structure refinement data are summarized in Table 1. The CIF file has been deposited with CCDC-276229. Copies of the data can be obtained on request free of charge by quoting the publication citation and the deposition number via http://www.ccdc.cam.ac.uk/conts/retrieving.html (or from the Cambridge Crystallographic Data Centre, 12, Union Road, Cambridge, CB2 1EZ, UK; Fax: +44 1223 336033; e-mail: deposit@ccdc.cam.ac.uk).

**Physical Measurements.** $^{31}$P and $^{183}$W NMR spectra were recorded with a Bruker Model AVANCE 500 spectrometer at 202.46 and 20.835 MHz, respectively. The $^{31}$P NMR spectra were obtained in a 5 mm diameter NMR tube with a concentric capillary containing $D_2O$ for an instrumental lock. Chemical shifts are expressed in parts per million with respect to 85% (v/v) $H_3PO_4$. The $^{183}$W NMR spectra were obtained in a 10 mm diameter tube, and chemical shifts were referenced to 1 M $Na_2WO_4\cdot 2H_2O$ in $D_2O$. The $^{31}$P and $^{183}$W NMR spectra were measured at 25 °C. Cyclic voltammograms were recorded with a HUSO Model HECS-

Published on the web January 13, 2006; DOI 10.1246/bcsj.79.100

Table 1. Crystallographic Data and Results of Structure Refinements for $((C_2H_5)_4N)_4[(P_2O_7)W_{17}O_{51}]\cdot CH_3CN$

| | |
|---|---|
| Formula | $C_{34}H_{83}N_5O_{58}P_2W_{17}$ |
| FW | 4677.43 |
| Crystal System | Monoclinic |
| Space Group | $P2_1/n$ |
| $a$/Å | 16.1877(8) |
| $b$/Å | 22.103(1) |
| $c$/Å | 22.670(1) |
| $\beta$/° | 90.847(1) |
| $V$/Å$^3$ | 8110.3(7) |
| $Z$ | 4 |
| $Dx$/g cm$^{-3}$ | 3.83 |
| Temperature/K | 100(2) |
| $\theta$ range/° | 2.05–30.56 |
| $R_{int}$ | 0.0978 |
| No. unique reflections | 20877 |
| No. parameters | 1045 |
| $R1$ ($F_o^2 > 2.0\sigma(F_o^2)$)[a)] | 0.0682 |
| $wR2$ (all data)[b)] | 0.1549 |
| Goodness of fit (all data) | 1.202 |
| $\Delta/\sigma$ max | 0.002 |
| Max/min residue | 3.67/−5.65 |

a) $R1 = \Sigma||F_o| - |F_c||/\Sigma|F_o|$. b) $wR2 = \{\Sigma(w(F_o^2 - F_c^2)^2)/\Sigma(w(F_o)^2)\}^{1/2}$ where $w = 1/\{\sigma^2(F_o)^2 + (0.0500P)^2 + 267.4932P\}$ and $P = 0.33333\{(0,F_o^2)\,\max\} + (1 - 0.33333)F_c^2$.

311C potentiostat interfaced to a microcomputer-controlled system. A Tokai glassy carbon (GC-30S) with a diameter of 5.0 mm was used as a working electrode and a platinum wire served as the counter electrode. The potentials are referred to the redox potential of ferrocene (Fc)/ferrocenium ion ($Fc^+$) as an internal reference. Prior to each measurement, the GC electrode was polished manually with 0.25 μm diamond slurry and washed with distilled water. The solutions were deoxygenated with nitrogen. All of the voltammetric measurements were made at 25 ± 0.1 °C. A Thermo Nicolet Model Avatar 360 spectrophotometer was used to record IR spectra as KBr pellets. UV–visible spectra were recorded on a Hitachi Model U-3000 spectrophotometer. All of the chemicals were of analytical grade and were used without further purification. Stock solutions of W(VI) and P(V) were prepared by dissolving appropriate amounts of $Na_2WO_4\cdot 2H_2O$ and $Na_4P_2O_7\cdot 10H_2O$, respectively.

**Syntheses.** For comparative studies, $(n\text{-}Bu_4N)_4[(P_2O_7)Mo_{18}O_{54}]$ was prepared according to our previous method.[1]

**$(n\text{-}Bu_4N)_4[(P_2O_7)W_{17}O_{51}]$:** To a solution of 33 g of $Na_2WO_4\cdot 2H_2O$ (100 mmol) and 2.3 g of $Na_4P_2O_7\cdot 10H_2O$ (5 mmol) in 280 mL of warm water was added dropwise 26 mL of concd HCl with vigorous stirring. A suspension occurred upon the addition of HCl, and the next drop was added after the solution became clear. To a thus-obtained clear solution was added 200 mL of $CH_3CN$. To the resultant yellow solution was added 8 g of $n$-$Bu_4NBr$ to yield a heavy oily material. The yellow oily material was collected, and 70 mL of $CH_3CN$ was added to produce a clear yellow solution. Pale-yellow salts were precipitated by the addition of 5 mL of water with vigorous stirring, and the solution was allowed to stand for three hours at ambient temperature. The thus-obtained pale-yellow precipitate was collected by vacuum filtration, washed with water and ethanol, and air-dried (yield; 0.9 g). The salt was further purified by recrystallization from $CH_3CN$, and dried at 50 °C under vacuum. Found: C, 15.1; H, 2.8; N, 1.3%. Calcd for $(n\text{-}Bu_4N)_4[(P_2O_7)W_{17}O_{51}]$: C, 15.1; H, 2.9; N, 1.1%. IR (KBr, cm$^{-1}$): 1163, 1100, 983, 919, 896, 788, 522, 494 (Fig. 1); the 1163 and 1100 cm$^{-1}$ bands are assigned to the $P_2O_7$ group. The $n$-$Bu_4N^+$ crystal was not suitable for X-ray intensity collection, owing to the hygroscopic character and the twinning of crystals.

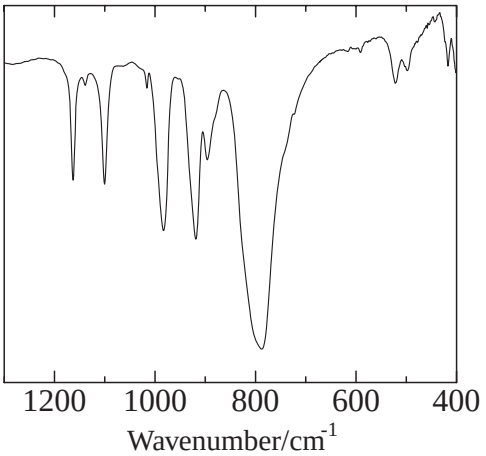


Fig. 1. An IR spectrum of $(n\text{-}Bu_4N)_4[(P_2O_7)W_{17}O_{51}]$ in the KBr pellet. Numerical data are given in the text.

In order to obtain crystals suitable for X-ray structural analysis, an aliquot of $(n\text{-}Bu_4N)_4[(P_2O_7)W_{17}O_{51}]$ was dissolved in $CH_3CN$, and the addition of $(C_2H_5)_4NClO_4$ ($Et_4NClO_4$) yielded the $Et_4N^+$ salt. Suitable-quality crystals were obtained by recrystallization of the $Et_4N^+$ salt in $CH_3CN$ at ambient temperature. Found: C, 8.4; H, 1.9; N, 1.4%. Calcd for $(Et_4N)_4[(P_2O_7)W_{17}O_{51}]\cdot CH_3CN$: C, 8.7; H, 1.8; N, 1.5%.

## Results and Discussion

**Crystal Structure Determination.** An ORTEP[11] diagram along with atomic numbering and a polyhedral model of the anion are shown in Fig. 2. The anion consists of 17 tungstate groups, one square pyramidal and the others octahedral, and one bent, eclipsed diphosphate group. In the anion, two $PW_8O_{31}$ units, which are each derived from the $\beta$-Keggin-type $[PW_{12}O_{40}]^{3-}$ anion by removing one "unrotated" $W_3O_6$ group (as B-$\beta$-$PW_9O_{34}$) and one $WO_3$ group adjacent to the removed $W_3O_{13}$ group in the "rotated" $W_3O_{13}$ unit, are linked by four W–O–W bridges (W3–O48–W11, W7–O49–W15, W8–O50–W16, and W6–O51–W14) and one P–O–P bridge (P1–O58–P2) to form an open, inkpot shaped $(P_2O_7)W_{16}O_{50}$ structure. A W(W17)$O_5$ square pyramid caps the open space to complete the $[(P_2O_7)W_{17}O_{51}]^{4-}$ polyanion. The anion thus has approximately $C_{2v}$ symmetry. Figure 3 shows the $PW_8O_{31}$ unit, where octahedra with asterisks are removed from the $\beta$-Keggin structure.

Selected interatomic distances and bond angles are listed in Table 2. The bond lengths around the W atoms are comparable to those found in the usual polyoxotungstates. The W–O(–P) distances to ternary shared O atoms, O54 and O57 (2.332(10)–2.369(9) Å), are slightly shorter than those to quaternary shared, O52, O53, O55, and O56 (2.396(10)–2.647(10) Å), reflecting different environments. The P–O(–W) distances are also normal (1.504(11)–1.516(10) Å), whereas the P–O(–P) distances are rather long (1.613(10) and 1.624(10) Å for P1–O58 and P2–O58, respectively). The P–O(–W) distances

(1.504(11)–1.516(10) Å) are normal in comparison with the corresponding values for Keggin- and Dawson-type polyoxometalates, whereas the P–O(–P) distances are rather long (1.613(10) and 1.624(10) Å for P1–O58 and P2–O58, respectively). These P–O(–P) distances are remarkably longer than those found in $[(P_2O_7)Mo_{18}O_{54}]^{4-}$ (1.56–1.59 Å) and $[\{(P_2O_7)Mo_{15}O_{45}\}_2]^{8-}$ (1.53–1.65 Å).[2,6] In the $[\{(P_2O_7)Mo_{15}O_{45}\}_2]^{8-}$ structure, one P–O(–P) distance in the diphosphate group, which is encapsulated in the molybdate cages and has an almost linear conformation, is much longer than the other three, ranging over 1.53–1.57 Å, although no discussion on this observation is given in the literature.[6] Also, the long P–O(–P) distance is comparable to those found in $[(P_2O_7)Mo_6O_{18}(OH_2)_4]^{4-}$ (1.61–1.65 Å)[7] and $[(P_2O_7)_4W_{12}O_{36}]^{16-}$ (1.59–1.70 Å),[9] where the diphosphate group has a bent conformation. The long distance of W17–O58 (2.946(9) Å) and the bond valence,[12] calculated from the distance (0.063), indicate no chemical bond between these two atoms.

At the linkage of the two $PW_8O_{31}$ units, the W7–O49–W15 and W8–O50–W16 angles (155.5(6) and 155.0(6)°, respectively) are less acute than the W3–O48–W11 and W6–O51–W14 angles (134.0(6) and 134.6(6)°, respectively). The angles for the former two linkages are comparable to those for the W1–O15–W4, W2–O17–W5, W9–O37–W12, and W10–O39–W13 angles (160.7(7), 152.5(6), 161.4(7), and 153.3(6)°, respectively), where bridging O atoms can be viewed as linking edge-shared $W_2O_{10}$ groups.

The P–O–P angle varies, depending on the structural feature of compounds.[2] The P1–O58–P2 angle (132.2(6)°) in the present polyanion is larger by ca. 10° than those found in $[(P_2O_7)Mo_6O_{18}(OH_2)_4]^{4-}$ (122.6°)[7] and $[(P_2O_7)_4W_{12}O_{36}]^{16-}$ (119.6–123.8°),[9] but comparable to those found in e.g. $K_3NaP_2O_7 \cdot 4H_2O$ (131.4°),[13] $K_4P_2O_7 \cdot 3H_2O$ (130.2°),[14] $(CN_3H_6)_4P_2O_7 \cdot H_2O_2 \cdot 1.5H_2O$ (131.7 and 130.3°),[15] $K_3HP_2O_7 \cdot 3H_2O$ (132.8°),[16] $\beta$-$Ca_2P_2O_7$ (130.6 and 137.7°),[17] and $Na_4P_2O_7 \cdot$

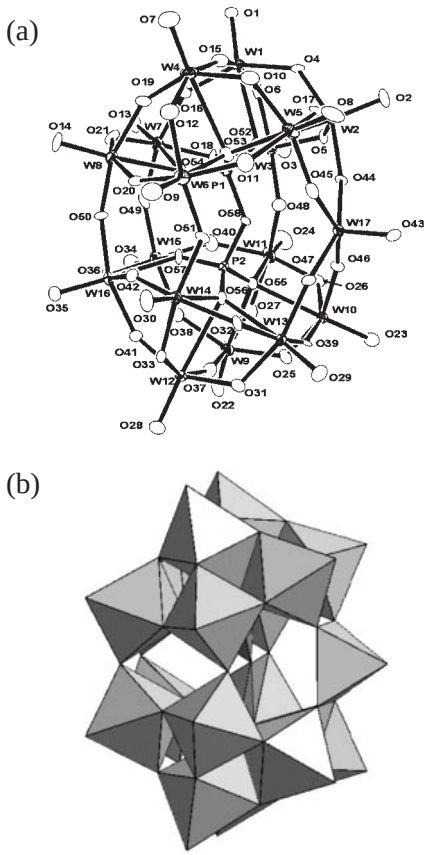


Fig. 2. An ORTEP view along with atomic notations (a) and a polyhedral representation (b) of the $[(P_2O_7)W_{17}O_{51}]^{4-}$ anion.

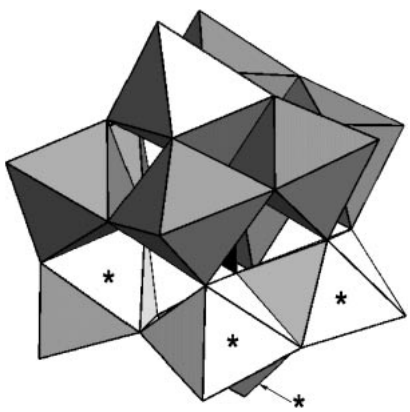

Fig. 3. Polyhedral representation of the $\beta$-Keggin structure, where octahedra marked with asterisks were removed to construct the present $[(P_2O_7)W_{17}O_{51}]^{4-}$ structure.

Table 2. Selected Interatomic Distances/Å and Bond Angles/° in $[(P_2O_7)W_{17}O_{51}]^{4-}$

| | | | | | |
|---|---|---|---|---|---|
| W1–O52 | 2.613(10) | W9–O55 | 2.637(10) | W17–O58 | 2.946(9) |
| W2–O52 | 2.400(10) | W10–O55 | 2.405(10) | P1–O52 | 1.516(10) |
| W3–O52 | 2.507(10) | W11–O55 | 2.479(10) | P1–O53 | 1.510(11) |
| W4–O53 | 2.644(11) | W12–O56 | 2.647(10) | P1–O54 | 1.512(10) |
| W5–O53 | 2.396(10) | W13–O56 | 2.396(10) | P1–O58 | 1.613(10) |
| W6–O53 | 2.486(10) | W14–O56 | 2.487(11) | P2–O55 | 1.504(11) |
| W7–O54 | 2.332(10) | W15–O57 | 2.349(10) | P2–O56 | 1.514(12) |
| W8–O54 | 2.358(9) | W16–O57 | 2.369(9) | P2–O57 | 1.505(10) |
| | | | | P2–O58 | 1.624(10) |

| | | | |
|---|---|---|---|
| W1–O15–W4 | 160.7(7) | W3–O48–W11 | 134.0(6) |
| W2–O17–W5 | 152.5(6) | W7–O49–W15 | 155.5(6) |
| W9–O37–W12 | 161.4(7) | W8–O50–W16 | 155.0(6) |
| W10–O39–W13 | 153.3(6) | W6–O51–W14 | 134.6(6) |
| | | P1–O58–P2 | 132.2(6) |

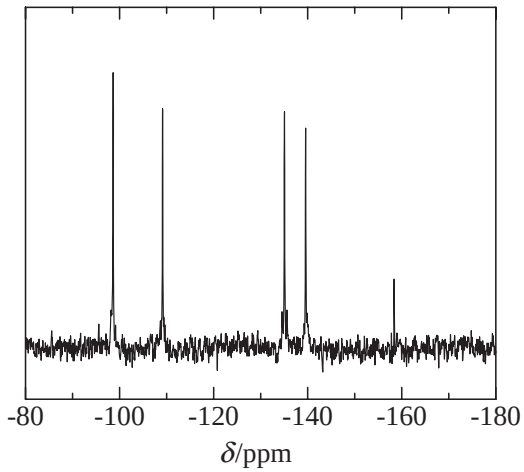


Fig. 4. A $^{183}$W NMR spectrum for $(n\text{-}Bu_4N)_4[(P_2O_7)W_{17}O_{51}]$ dissolved in $CD_3CN$. Numerical data are given in the text.

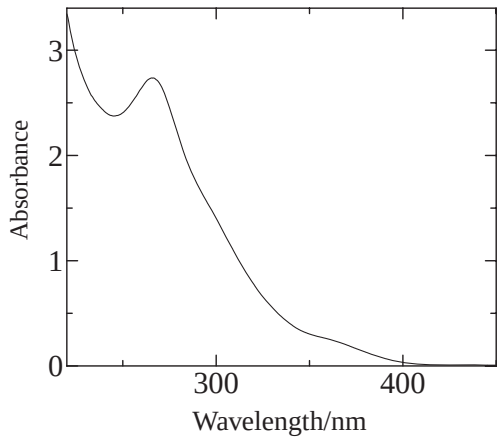


Fig. 5. A UV–vis spectrum for a $5.0 \times 10^{-5}$ M $[(P_2O_7)W_{17}O_{51}]^{4-}$ in $CH_3CN$. Path length; 1.0 cm.

$10H_2O$ (130.2°).[18] It should be added that the long P–O(–P) distances in the present polyanion are also comparable to those found in these salts of $P_2O_7^{4-}$ (1.57–1.66 Å).

**$^{183}$W and $^{31}$P NMR Spectra.** The $^{183}$W spectrum was recorded for the $n$-$Bu_4N^+$ salt of $[(P_2O_7)W_{17}O_{51}]^{4-}$ dissolved in 1:1 (v/v) $CH_3CN$–$CD_3CN$, because the solubility of the $Et_4N^+$ salt is not sufficiently high for the NMR measurement. The $n$-$Bu_4N^+$ salt is very soluble in $CH_3CN$ to give a pale-yellow solution. As shown in Fig. 4, the $^{183}$W NMR spectrum consisted of five lines at −98.6, −109.1, −135.0, −139.5, and −158.4 ppm with the respective intensity ratios of 4:4:4:4:1. The $^{183}$W NMR result for the $n$-$Bu_4N^+$ salt is consistent with the solid-state $[(P_2O_7)W_{17}O_{51}]^{4-}$ structure, which is further confirmed by the appearance of a single $^{31}$P NMR line at −22.1 ppm in $CH_3CN$. These results demonstrate that both $n$-$Bu_4N^+$ and $Et_4N^+$ crystals contain the same structure of $[(P_2O_7)W_{17}O_{51}]^{4-}$, and the structure is retained in $CH_3CN$.

**UV–Vis Spectra.** Figure 5 shows the UV–vis spectrum for a $5.0 \times 10^{-5}$ M solution of $[(P_2O_7)W_{17}O_{51}]^{4-}$ in $CH_3CN$. The UV–vis spectrum is characterized by an absorption maximum at 266 nm; the molar extinction coefficient ($\varepsilon_{max}$) was found to be $5.42 \times 10^4$ mol$^{-1}$ dm$^3$ cm$^{-1}$ at this wavelength. The

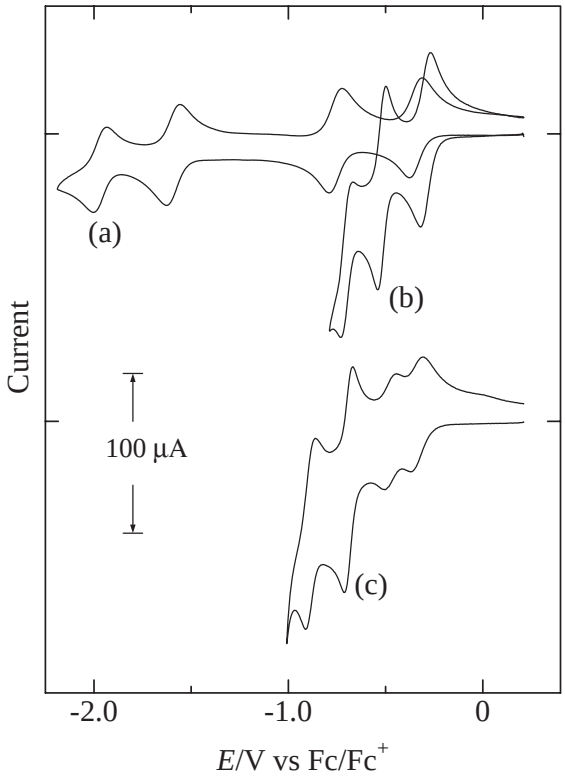


Fig. 6. Cyclic voltammograms of 0.50 mM $[(P_2O_7)W_{17}O_{51}]^{4-}$ in $CH_3CN$ containing (a) 0.10 M $n$-$Bu_4NClO_4$; (b) (a) +10 mM $H^+$; (c) (b) +2% (v/v) $H_2O$.

$[(P_2O_7)W_{17}O_{51}]^{4-}$ anion is kinetically stable in $CH_3CN$, as judged by no spectral change with time, and the UV–vis spectrum conformed to Beer's law in the spectra region studied.

**Voltammetric Characterization.** The electrochemical properties of polyoxometalates are of increasing interest owing to their potential use in redox catalysis.[19] We have already synthesized $[(P_2O_7)Mo_{18}O_{54}]^{4-}$ from an analogous system of 50 mM Mo(VI)–5 mM $P_2O_7^{4-}$–0.7 M HCl–60% (v/v) $CH_3CN$.[1] Both $[(P_2O_7)W_{17}O_{51}]^{4-}$ and $[(P_2O_7)Mo_{18}O_{54}]^{4-}$ anions have the same charge of −4, but their structures are entirely different.[2] Cyclic voltammograms for $[(P_2O_7)W_{17}O_{51}]^{4-}$ and $[(P_2O_7)Mo_{18}O_{54}]^{4-}$ were compared in order to correlate their structures and electrochemical properties.

Figure 6a shows a cyclic voltammogram of 0.50 mM $[(P_2O_7)W_{17}O_{51}]^{4-}$ in $CH_3CN$ containing 0.10 M $n$-$Bu_4NClO_4$. Four one-electron redox waves were obtained with mid-point potentials ($E_{mid}$) of −0.35, −0.76, −1.59, and −1.97 V, where $E_{mid} = (E_{pc} - E_{pa})/2$; $E_{pc}$ and $E_{pa}$ are the cathodic and anodic peak-potentials, respectively. The separation of the $E_{pc}$ and $E_{pa}$ values for each redox couple averaged 61 mV, and the peak-potentials ($E_p$'s) were independent of the voltage scan rate (50–200 mV/s), indicating the reversible nature of each wave. As already described,[20] $[(P_2O_7)Mo_{18}O_{54}]^{4-}$ underwent a four-step reversible one-electron reduction with $E_{mid}$ values of −0.04, −0.24, −0.84, and −1.15 V.

With the addition of acid, as shown in Fig. 6b, the one-electron waves were converted into three two-electron waves with $E_{mid}$ values of −0.30, −0.52, and −0.70 V. The peak-separation for each redox wave averaged 45 mV, and the first reduc-

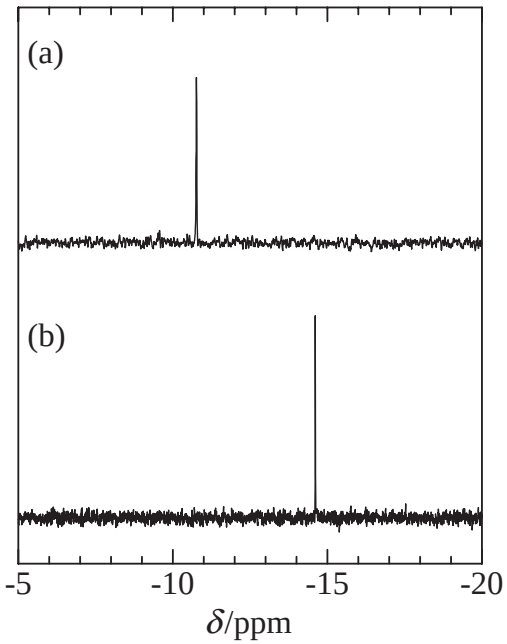


Fig. 7. $^{31}$P NMR spectra for an aqueous 50 mM W(VI)–10 mM $P_2O_7^{4-}$–0.6 M HCl system. Recorded after standing at room temperature for (a) 30 min; (b) three days.

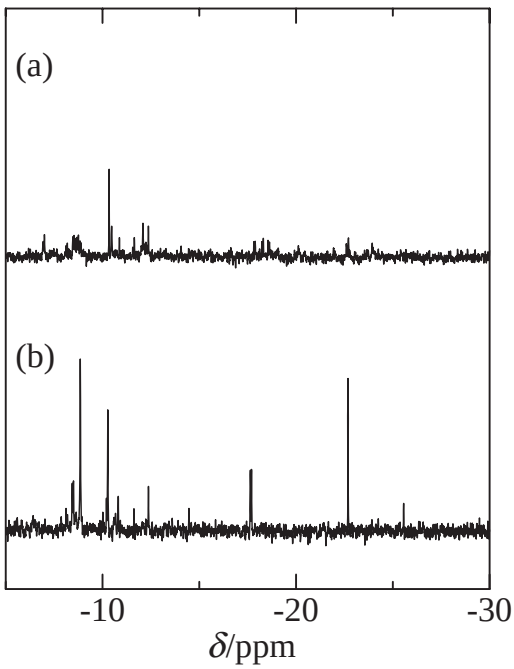


Fig. 8. $^{31}$P NMR spectra for a 200 mM W(VI)–10 mM $P_2O_7^{4-}$–0.6 M HCl system; (a) without and (b) with 40% (v/v) $CH_3CN$. Recorded after standing at room temperature for 60 min.

tion current was approximately twice the original one-electron reduction current. According to Polcyn and Shain,[21] this behavior occurs when the first two one-electron waves are reduced at nearly the same potential. For Keggin and Dawson anions, the two-electron reduction is accompanied by the consumption of two protons in the electrode process.[22–26] Similarly, the two-electron redox behavior of $[(P_2O_7)W_{17}O_{51}]^{4-}$ can be accounted for in terms of protonation of the electrochemically reduced species at the electrode surface.

Upon the addition of $H_2O$, the first two-electron wave can be converted into two one-electron waves for $\alpha$- and $\beta$-$[PW_{12}O_{40}]^{3-}$ and $\alpha$-$[S_2W_{18}O_{62}]^{4-}$ in acidified $CH_3CN$[27,28] and for $\alpha$-$[PMo_{12}O_{40}]^{3-}$ in $CH_3CN$ containing $Li^+$.[29] These voltammetric behaviors are explained by the preferential solvation of $H^+$ or $Li^+$ by $H_2O$ in a binary mixture of $H_2O$ and $CH_3CN$.[29,30] In order to study the effect of $H_2O$ on the voltammetric behavior of $[(P_2O_7)W_{17}O_{51}]^{4-}$, the cyclic voltammogram was recorded again after the addition of 2% (v/v) $H_2O$. As shown in Fig. 6c, the first two-electron wave was converted back into two one-electron waves, and consequently successive one-, one-, two-, and two-electron redox waves were obtained.

**Formation of $[(P_2O_7)W_{17}O_{51}]^{4-}$ in a W(VI)–$P_2O_7^{4-}$–HCl–$CH_3CN$ System.** In order to clarify the formation of $[(P_2O_7)W_{17}O_{51}]^{4-}$, $^{31}$P NMR spectra were recorded for an aqueous 50 mM W(VI)–10 mM $P_2O_7^{4-}$–0.6 M HCl system. When $^{31}$P NMR spectra were measured after the system was left standing for 30 min at room temperature, as shown in Fig. 7a, we found a $^{31}$P NMR line at $-10.8$ ppm, due to the unreacted $P_2O_7^{4-}$ ion. As time passed, the $^{31}$P NMR spectrum showed a new line at $-14.6$ ppm (Fig. 7b), indicating that diphosphate, $P_2O_7^{4-}$ undergoes hydrolytic degradation to orthophosphate to form an $\alpha$-Keggin-type $[PW_{12}O_{40}]^{3-}$ complex.[31] When the W(VI) concentration was increased to 200 mM, as shown in Fig. 8a, we found many minor $^{31}$P NMR lines at both the upfield and downfield sides of the $P_2O_7^{4-}$ line. However, no evidence was obtained for the formation of $[(P_2O_7)W_{17}O_{51}]^{4-}$ in any appreciable amount.

When the $^{31}$P NMR spectra were measured in the presence of 40% (v/v) $CH_3CN$, we found a large $^{31}$P NMR line at $-22.6$ ppm in addition to the unidentified lines (Fig. 8b), indicating the formation of $[(P_2O_7)W_{17}O_{51}]^{4-}$. As described above, the structure of the solution species is consistent with the solid-state structure. The $-22.6$ ppm line persisted for seven days at room temperature. When measurements were made after heating the solution at 60 °C for two days, however, the $-22.6$ ppm line disappeared completely with the appearance of $^{31}$P NMR lines due to $\alpha$-$[PW_{12}O_{40}]^{3-}$ and $\alpha$-$[P_2W_{18}O_{62}]^{6-}$ (at $-12.3$ ppm), along with some of the unidentified $^{31}$P NMR lines. For $P_2O_7^{4-}$ concentrations of $<10$ mM, the $[(P_2O_7)W_{17}O_{51}]^{4-}$ complex inevitably coexists with several isopolyoxotungstates.[32] At higher concentrations of $P_2O_7^{4-}$, on the other hand, a mixture of $[(P_2O_7)W_{17}O_{51}]^{4-}$ and $\alpha$-$[PW_{12}O_{40}]^{3-}$ was precipitated as the $n$-$Bu_4N^+$ salts. Since a turbidity occurred at $CH_3CN$ concentrations $>$ 50% (v/v), the 200 mM W(VI)–10 mM $P_2O_7^{4-}$–0.6 M HCl–40% (v/v) $CH_3CN$ system was chosen as being optimum for the preparation of $[(P_2O_7)W_{17}O_{51}]^{4-}$.

## Conclusion

A novel diphosphoheptadecatungstate complex, $[(P_2O_7)W_{17}O_{51}]^{4-}$ was prepared from a 200 mM W(VI)–10 mM $P_2O_7^{4-}$–0.6 M HCl–40% (v/v) $CH_3CN$ system. The $^{31}$P NMR study showed that the presence of $CH_3CN$ at 40–50% (v/v) is essential for its formation.

Cyclic voltammograms for $[(P_2O_7)W_{17}O_{51}]^{4-}$ and $[(P_2O_7)$-

$Mo_{18}O_{54}]^{4-}$ were compared in $CH_3CN$. Both $[(P_2O_7)W_{17}O_{51}]^{4-}$ and $[(P_2O_7)Mo_{18}O_{54}]^{4-}$ anions have common properties of undergoing a four-step reversible one-electron reduction in $CH_3CN$. The one-electron redox behavior is consistent with Pope's rule, because each of the $MO_6$ octahedra in the peripheral structure of $[(P_2O_7)W_{17}O_{51}]^{4-}$ and $[(P_2O_7)Mo_{18}O_{54}]^{4-}$ has one terminal oxygen atom.

In the presence of acid, $[(P_2O_7)W_{17}O_{51}]^{4-}$ undergoes a three-step two-electron reduction, and the presence of $H_2O$ causes the first two-electron wave to be converted into two one-electron waves. The voltammetric behavior of $[(P_2O_7)W_{17}O_{51}]^{4-}$ is similar to those of the Keggin and Dawson anions, and is quite unlike that of $[(P_2O_7)Mo_{18}O_{54}]^{4-}$. In the presence of acid, $[(P_2O_7)Mo_{18}O_{54}]^{4-}$ undergoes a four-electron reduction, followed by two two-electron reductions,[20] and the presence of 5% (v/v) water causes the four-electron wave to split into two two-electron waves.[8] From these findings it follows that the two- and four-electron behaviors are not directly related to the structures of polyoxometalates, but to the protonation of their reduced forms at the electrode surface.

The authors are grateful to Dr. Yoshihito Hayashi at Department of Chemistry, Faculty of Science, Kanazawa University for his kind help to collect X-ray intensity data.

## References

1 S. Himeno, A. Saito, T. Hori, *Bull. Chem. Soc. Jpn.* **1990**, *63*, 1602.
2 U. Kortz, M. T. Pope, *Inorg. Chem.* **1994**, *33*, 5643.
3 S. Himeno, T. Kubo, A. Saito, T. Hori, *Inorg. Chim. Acta* **1995**, *236*, 167.
4 S. Himeno, T. Ueda, M. Shiomi, T. Hori, *Inorg. Chim. Acta* **1997**, *262*, 219.
5 A. Rosenheim, M. Schapiro, *Z. Anorg. Chem.* **1923**, *129*, 196.
6 U. Kortz, *Inorg. Chem.* **2000**, *39*, 623.
7 U. Kortz, *Inorg. Chem.* **2000**, *39*, 625.
8 S. Himeno, A. Saito, *J. Electroanal. Chem.* **1995**, *391*, 207.
9 U. Kortz, G. B. Jameson, M. T. Pope, *J. Am. Chem. Soc.* **1994**, *116*, 2659.
10 G. M. Sheldrick, *SHELX97*, University of Göttingen, Germany, **1997**.
11 C. K. Johnson, *ORTEPII. Report ORNL-5138*, Oak Ridge National Laboratory, Tennessee, U.S.A., **1976**.
12 I. D. Brown, D. Altermatt, *Acta Crystallogr., Sect. B* **1985**, *41*, 244.
13 Y. Dumas, A. Escande, J. L. Galigne, *Acta Crystallogr., Sect. B* **1978**, *34*, 710.
14 Y. Dumas, J. L. Galigne, *Acta Crystallogr., Sect. B* **1974**, *30*, 390.
15 J. M. Adams, V. Ramdas, *Acta Crystallogr., Sect. B* **1978**, *34*, 2150.
16 Y. Dumas, J. L. Galigne, J. Falgueilettes, *Acta Crystallogr., Sect. B* **1973**, *29*, 1623.
17 N. C. Webb, *Acta Crystallogr.* **1966**, *21*, 942.
18 W. S. McDonald, D. W. J. Cruickshank, *Acta Crystallogr.* **1967**, *22*, 43.
19 M. Sadakane, E. Steckhan, *Chem. Rev.* **1998**, *98*, 219.
20 S. Himeno, M. Takamoto, *J. Electroanal. Chem.* **2000**, *492*, 63.
21 D. S. Polcyn, I. Shain, *Anal. Chem.* **1966**, *38*, 370.
22 D. M. Way, J. B. Cooper, M. Sadek, T. Vu, P. J. Mahon, A. M. Bond, R. T. C. Brownlee, A. G. Wedd, *Inorg. Chem.* **1997**, *36*, 4227.
23 P. D. Prenzler, C. Boskovic, A. M. Bond, A. G. Wedd, *Anal. Chem.* **1999**, *71*, 3650.
24 P. J. Richardt, R. W. Gable, A. M. Bond, A. G. Wedd, *Inorg. Chem.* **2001**, *40*, 703.
25 A. M. Bond, T. Vu, A. G. Wedd, *J. Electroanal. Chem.* **2000**, *494*, 96.
26 S. Himeno, M. Takamoto, R. Santo, A. Ichimura, *Bull. Chem. Soc. Jpn.* **2005**, *78*, 95.
27 S. Himeno, M. Takamoto, T. Ueda, *J. Electroanal. Chem.* **1999**, *465*, 129.
28 S. Himeno, H. Tatewaki, M. Hashimoto, *Bull. Chem. Soc. Jpn.* **2001**, *74*, 1623.
29 M. Takamoto, T. Ueda, S. Himeno, *J. Electroanal. Chem.* **2002**, *521*, 132.
30 S. Himeno, M. Takamoto, T. Ueda, R. Santo, A. Ichimura, *Electroanalysis* **2004**, *16*, 656.
31 S. Himeno, M. Takamoto, T. Ueda, *Bull. Chem. Soc. Jpn.* **2005**, *78*, 1463.
32 S. Himeno, M. Yoshihara, M. Maekawa, *Inorg. Chim. Acta* **2000**, *298*, 165.